J. Phys. Chem. 1994, 98, 5801–5806

ARTICLES

Iminoethenone Radical Cations ($RN{=}C{=}C{=}O^{\bullet+}$): Tandem Mass Spectrometry and ab Initio MO Studies

Robert Flammang,* Yves Van Haverbeke, Sophie Laurent, and Monique Barbieux-Flammang

Department of Organic Chemistry, University of Mons-Hainaut, B-7000 Mons, Belgium

Ming Wah Wong* and Curt Wentrup*

Department of Chemistry, The University of Queensland, Brisbane, Queensland 4072, Australia

*Received: November 22, 1993; In Final Form: April 4, 1994**

Radical cations of iminoethenone, $RN{=}C{=}C{=}O^{\bullet+}$ (R = H and CH_3), have been generated by dissociative ionization of isoxazolopyrimidine precursors and structurally characterized by collisional activation mass spectrometry. Contrasting with the behavior of their sulfur analogues, vertical electron transfer in a neutralization experiment does not result in the formation of observable $RN{=}C{=}C{=}O$ neutrals. This finding is in excellent accord with high-level ab initio calculations at the G2(MP2) level of theory. Although both HNCCO (**2**) and CH_3NCCO (**4**) are calculated to be stable equilibrium structures, dissociation into HNC (or CH_3NC) + CO require activation energies of only ~10 kJ mol^{-1}. Both **2** and **4** are predicted to have a singlet ground state, 78 and 83 kJ mol^{-1}, respectively, below the triplet. Iminoethenone radical cation ($2^{\bullet+}$) is predicted to be the lowest-energy C_2HNO^+ ion and is stable toward all possible fragmentations: the most favorable fragmentations into $H^\bullet$ + $NCCO^+$ and HNC + $CO^{\bullet+}$ are in accord with the mass spectrometric observations.

1. Introduction

Heterocumulenes derived from dicarbon, $X{=}C{=}C{=}Y$ (X, Y = O or S), have received considerable attention in recent years. C=C occurs in a variety of chemical reactions and in a wide range of astrophysical objects.[1] Thioxoethylidene, $:C{=}C{=}S$, a molecule of cosmochemical interest, has also been the subject of numerous publications.[2] Despite intensive research, ethenedione, $O{=}C{=}C{=}O$, has not yet been observed experimentally.[3] In contrast, ethenedithione, $S{=}C{=}C{=}S$, has been produced and unambiguously identified in matrix isolation,[4,5] flash-vacuum pyrolysis,[4,5] and neutralization–reionization experiments.[6] Neutral $O{=}C{=}C{=}S$ has been produced in the gas phase by reduction of the corresponding radical cations.[7]

Very recently, we have characterized ionized and neutral iminoethenethiones, $RN{=}C{=}C{=}S$,[8] by tandem mass spectrometry methods such as collisional activation (CA)[9] and neutralization–reionization (NR)[10] mass spectrometry.

Here, we report the studies on a new class of heterocumulenes, the monoimines of ethenedione, $RN{=}C{=}C{=}O$ (R = H and CH_3), using a combination of mass spectrometry-based experiments and high-level ab initio molecular orbital calculations[11] at the G2(MP2) level of theory.[12]

2. Mass Spectrometry

$HN{=}C{=}C{=}O^{\bullet+}$ ($2^{\bullet+}$) and $HN{=}C{=}C{=}O$ (2). $[C_2,H,N,O]^{\bullet+}$ radical cations can be generated by dissociative ionization of various oxygenated analogs of purine. For instance, the 70-eV electron impact mass spectrum of 3-phenylisoxazolo[4,5-*d*]-pyrimidine-5,7-(4*H*,6*H*)-dione (**1**) features a signal of moderate intensity at *m/z* 55 (12%) (Scheme 1). The CA spectrum of this ion using helium as the collision gas is shown in Figure 1a. The $HN{=}C{=}C{=}O$ connectivity is clearly indicated by peaks at *m/z* 40 (loss of NH), *m/z* 38 ($[C{=}C{=}N]^{\bullet+}$ ions), and *m/z* 27 (loss of CO). This loss of CO is the direct bond cleavage of the lowest-energy requirement in agreement with thermochemical predictions (eqs 1 and 2):[13]

$$\Delta H_f^\circ(HNC^{\bullet+}) + \Delta H_f^\circ(CO) = 1297 \text{ kJ mol}^{-1} \quad (1)$$

$$\Delta H_f^\circ(HNC) + \Delta H_f^\circ(CO^{\bullet+}) = 1442 \text{ kJ mol}^{-1} \quad (2)$$

That $HNC^{\bullet+}$ ions are produced in the *m/z* 55 → *m/z* 27 fragmentation is clearly demonstrated by a double-collision experiment on the *m/z* 27 ions generated by collision-induced dissociation of the *m/z* 55 ions. The significant fragments at *m/z* 12 and 15 characterize $HNC^{\bullet+}$, not $HCN^{\bullet+}$ (Figure 2).[14]

Figure 1b shows the CA spectrum of the $HN{=}C{=}C{=}O^{\bullet+}$ ($2^{\bullet+}$) ions using oxygen as the collision gas. The relative abundances of the peaks are quite similar to those observed with helium, except for a strong increase in intensity at *m/z* 41 corresponding to the loss of a nitrogen atom. Such behavior is completely unexpected and could be due to a post-collisional rearrangement by a 1,2-hydrogen shift into an ionized nitrene, $H(N)C{=}C{=}C{=}O^{\bullet+}$.[15] Production of formyl cyanide ions, $H{-}CO{-}CN^{\bullet+}$, seems unlikely on thermochemical grounds[13] as the most favorable cleavage should produce $HCO^{\bullet+}$ + CN.[15c] An MS/MS/MS experiment performed on the *m/z* 41 ions is shown in Figure 3. This spectrum is very similar to that of the *m/z* 41 ions from acetone, which one would expect to have the structure $HCCO^+$. However, both of these CA spectra of *m/z* 41 feature strong signals at *m/z* 29, corresponding to the loss of a carbon atom, whereas the peak at *m/z* 13 signifies the presence of CH. We believe that the loss of a carbon atom from *m/z* 41 is due to a post-collisional isomerization; an indication of this is found in the NRMS of these *m/z* 41 ions, which features significant

* Abstract published in *Advance ACS Abstracts*, May 1, 1994.

0022-3654/94/2098-5801$04.50/0

SCHEME 1

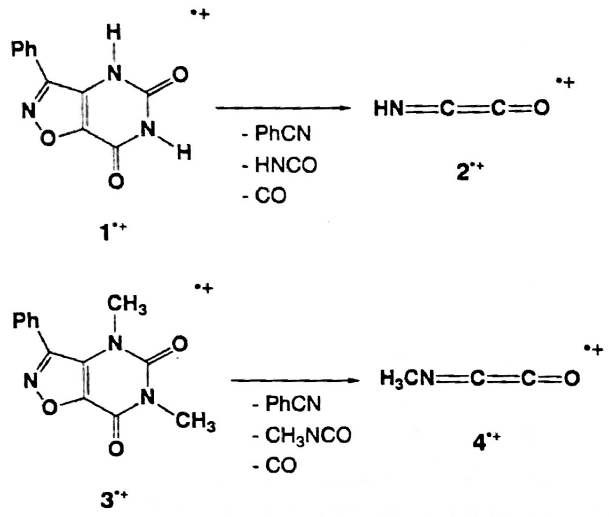

signals at m/z 13 and 28 but a much reduced one at m/z 29. It is our experience with other systems that ions not obviously related to the structures (i.e., ions formed in isomerization reactions) have much reduced intensities in the NRMS.[15a,b]

Another proof of the NCCO connectivity of the m/z 55 ions from $\mathbf{1}^{\bullet+}$ arises from a careful examination of the fragment at m/z 54. Using CA and NR mass spectra, McGibbon et al. have very recently shown that N=C=C=O$^+$, C=N=C=O$^+$, and C=C=N=O$^+$ ions are stable and distinct species in the gas phase.[16] These closed-shell ions have been synthesized by dissociative ionization of pyruvonitrile (CH_3–CO–CN), methyl isocyanate (CH_3NCO), and dichloroglyoxime (HON=C(Cl)C(Cl)=NOH), respectively. Figure 4 shows the CA and NR mass spectra of the m/z 54 ions produced from $\mathbf{1}^{\bullet+}$ which are in very good agreement with the data published for pyruvonitrile,[16] thus indicating the NCCO connectivity.

The NR mass spectrum of HN=C=C=O$^{\bullet+}$ ($\mathbf{2}^{\bullet+}$) ions does not present any significant recovery signal at m/z 55 corresponding to survivor ions (Figure 1c). The base peak at m/z 28 probably results from reionization of CO lost by collisional activation of the ions in the neutralization cell and fragmentation of neutral HN=C=C=O (**2**) between the cells,[17] whereas the other peaks can be attributed to reionization and fragmentation of NCCO radicals. It thus appears that, just like in the C_2O_2 case,[3g,h] vertical electron transfer in a neutralization experiment does not result in the formation of observable HN=C=C=O neutrals.

CH_3N=C=C=O$^{\bullet+}$ ($\mathbf{4}^{\bullet+}$) and CH_3N=C=C=O (4). The behavior of 4,6-dimethyl-3-phenylisoxazolo[4,5-*d*]pyrimidine-5,7-dione (**3**) upon electron impact is identical to that of the parent heterocycle **1**, except for an increased abundance of the ions of interest, $[C_3,H_3,N,O]^{\bullet+}$ (m/z 69, 88%) (Scheme 1). The CA (He) spectrum (Figure 5a) of these ions is characterized by peaks at m/z 54 (loss of 15 amu) and m/z 15, indicating the presence of a methyl group. This is confirmed by using the isotopomer ions, $[C_3,D_3,N,O]^{\bullet+}$, produced from the bis(trideuteriomethyl)-pyrimidinedione (**3D**). The base peak at m/z 41 corresponds to $CH_3NC^{\bullet+}$ ions as expected on thermochemical grounds (eqs 3 and 4):[13]

$$\Delta H_f°(CH_3NC^{\bullet+}) + \Delta H_f°(CO) = 1147 \text{ kJ mol}^{-1} \quad (3)$$

$$\Delta H_f°(CH_3NC) + \Delta H_f°(CO^{\bullet+}) = 1414 \text{ kJ mol}^{-1} \quad (4)$$

These fragmentations establish the CH_3N=C=C=O connectivity of the m/z 69 radical cations, which are cumulogs[18] of nitrosomethane ions. Note that, in this case, the CA spectrum is not significantly modified by using oxygen as the collision gas.

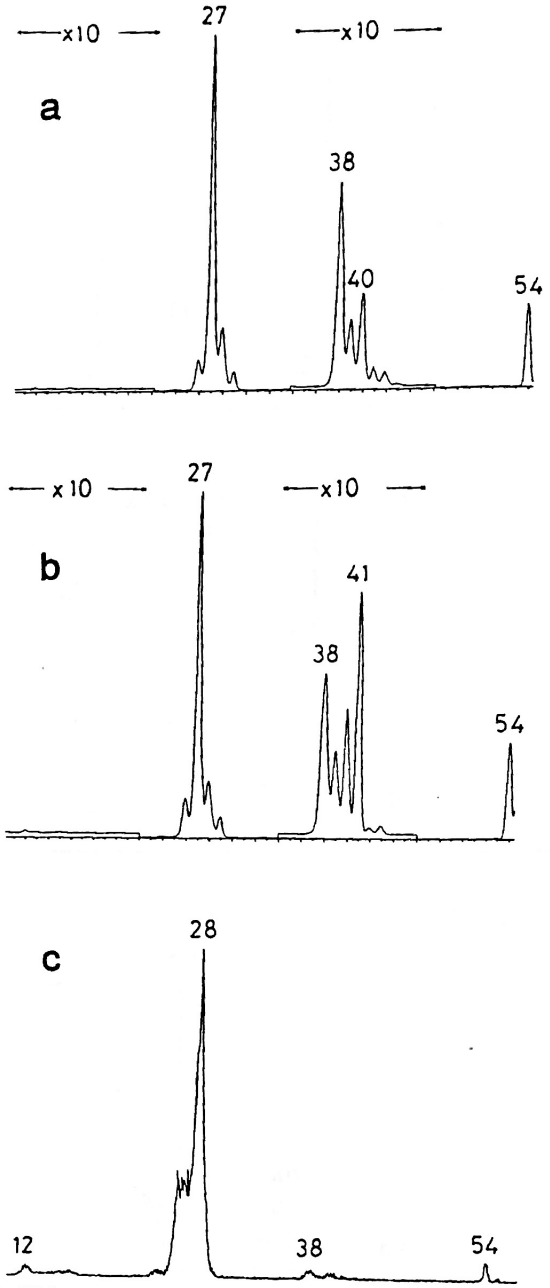

Figure 1. HN=C=C=O$^{\bullet+}$ ions ($\mathbf{2}^{\bullet+}$) (m/z 55) from $\mathbf{1}^{\bullet+}$: (a) CA (He) mass spectrum, (b) CA (O_2) mass spectrum, and (c) NR mass spectrum.

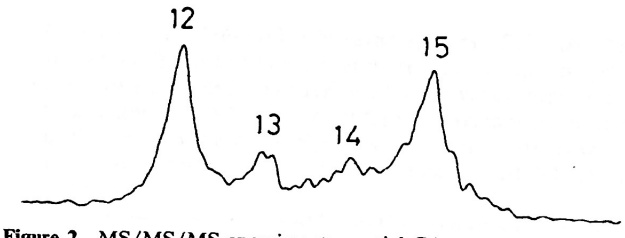

Figure 2. MS/MS/MS experiment: partial CA spectrum of m/z 27 ($HNC^{\bullet+}$) ions produced by collisional activation of m/z 55 ions from $\mathbf{1}^{\bullet+}$.

The major difference is seen in the doubly-charged ion region dominated by $HCNCCO^{2+}$ dications (m/z 33.5) (Figure 5b).[19]

The NR mass spectrum (Figure 5c) of CH_3N=C=C=O$^{\bullet+}$ ($\mathbf{4}^{\bullet+}$) does not present any recovery signal at m/z 69. The peak at m/z 54 probably corresponds to the reionization of NCCO radicals formed in the neutralization cell. Again, vertical electron transfer does not result in the formation of observable CH_3N=C=C=O neutrals (**4**).

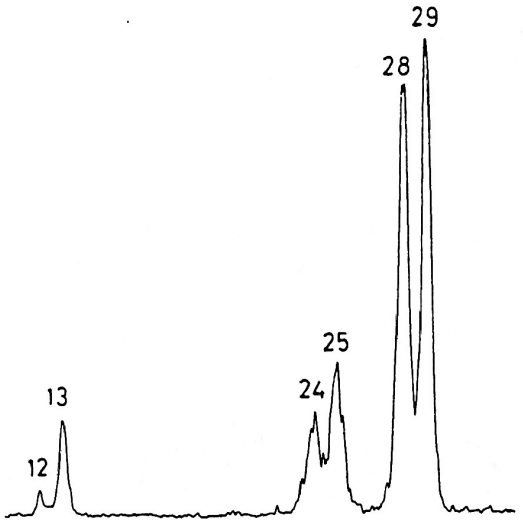

Figure 3. MS/MS/MS experiment: partial CA spectrum of m/z 41 ions produced by collisional activation (O_2) of m/z 55 ions from $\mathbf{1}^{\bullet+}$.

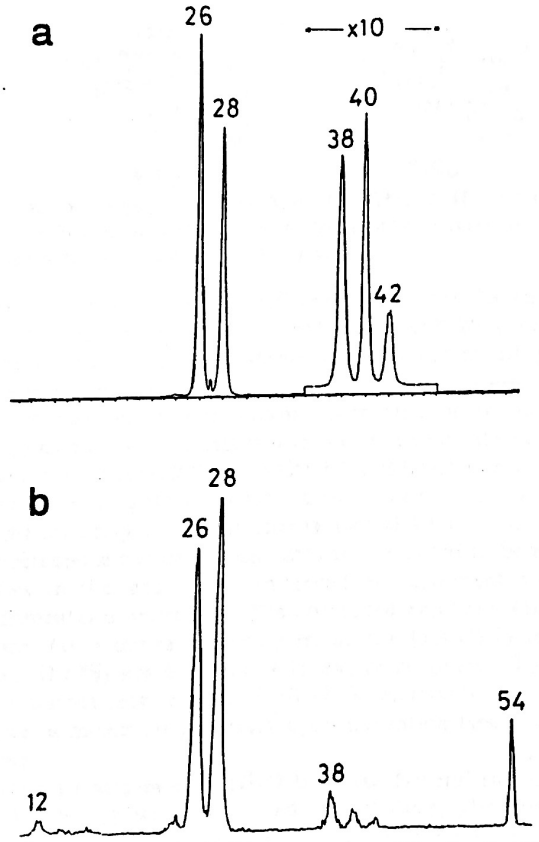

Figure 4. CA (O_2) (a) and NR (b) mass spectra of $N{\equiv}C{-}C{\equiv}O^+$ ions (m/z 54) from $HN{\equiv}C{-}C{\equiv}O^{\bullet+}$ ($\mathbf{2}^{\bullet+}$, m/z 55).

3. Theory

Method and Results. Standard ab initio molecular orbital calculations[11] were carried out using the GAUSSIAN 92 series of programs.[20] The structures and energies of C_2HNO, $C_2HNO^{\bullet+}$, and C_3H_3NO were investigated by the Gaussian-2 [G2(MP2)] theory. The G2(MP2) method, described in detail elsewhere,[12] is a composite procedure based effectively on QCISD(T)/6-311+G(3df,2p)//MP2/6-31G* energies (evaluated by making certain additivity assumptions) together with zero-point vibrational and isogyric corrections. In the G2(MP2) theory, the basis set extension energy corrections are obtained at the MP2 level.[12a] Optimized MP2/6-31G* geometries for $C_2HNO^{\bullet+}$, C_2HNO, and C_3H_3NO isomeric structures and transition structures are displayed in Figure 6, with corresponding G2(MP2) total and relative energies summarized in Table 1.

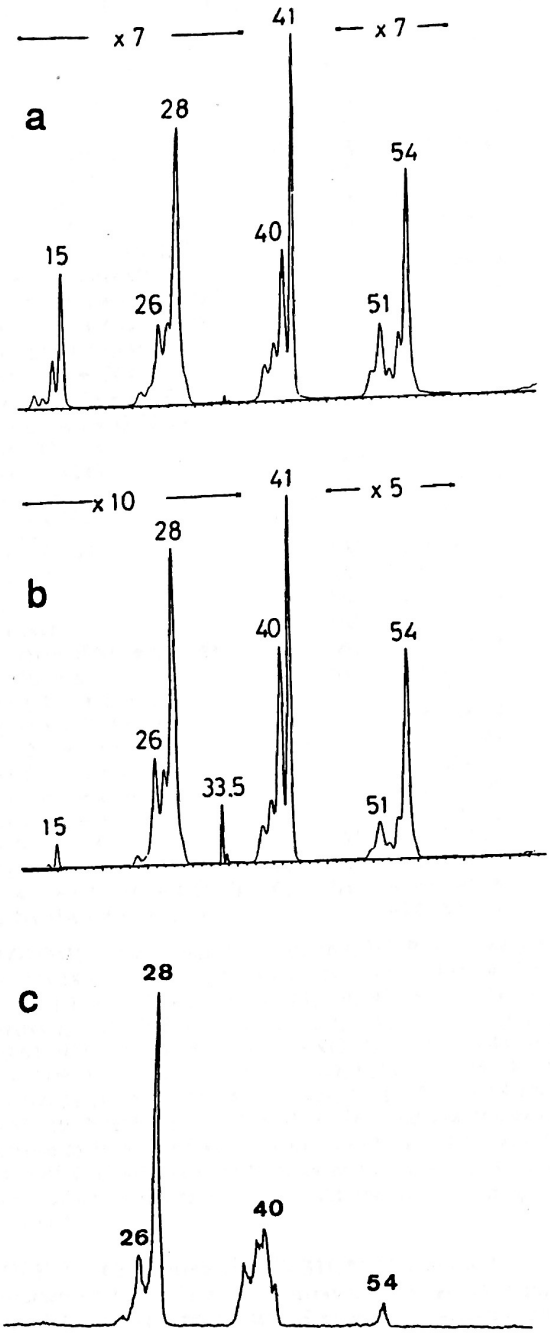

Figure 5. CA (He, a) (O_2, b), and NR (c) mass spectra of $CH_3N{\equiv}C{-}C{\equiv}O^{\bullet+}$ ions (m/z 69) from $\mathbf{3}^{\bullet+}$.

Calculated (HF/6-31G*) infrared spectra of singlet (**2S**) and triplet (**2T**) iminoethenone and its radical cation ($\mathbf{2}^{\bullet+}$) are presented in Table 2. The HF/6-31G* wavenumbers were scaled by a factor of 0.8929 to account for their average overestimation at this level of theory.[21] Spin-restricted calculations were used for closed-shell systems and spin-unrestricted for open-shell systems.

Structure and Stability of $HN{\equiv}C{-}C{\equiv}O^{\bullet+}$ and Isomeric Ions. Iminoethenone radical cation ($\mathbf{2}^{\bullet+}$) is predicted to be the lowest-energy structure of the composition $C_2HNO^{\bullet+}$. $HCNCO^{\bullet+}$ is the next most stable isomer, 16 kJ mol^{-1} above $\mathbf{2}^{\bullet+}$. Interestingly, the nitrene radical cation, $H(N)CCO^{\bullet+}$, also lies close in energy, 35 kJ mol^{-1} less stable than $\mathbf{2}^{\bullet+}$. $H{-}CO{-}CN^{\bullet+}$, $HOCCN^{\bullet+}$, and $HCCNO^+$ are significantly higher in energy (Table 1). The cumulene ion ($\mathbf{2}^{\bullet+}$) is predicted to have a W-shaped skeleton (Figure 6). It has strongly localized C≡N and C≡O bonds (1.165 and 1.143 Å, respectively). For comparison, the MP2/6-31G* C≡N and C≡O bond lengths in HCN and CO are 1.176 and 1.150 Å, respectively. The calculated C–C bond

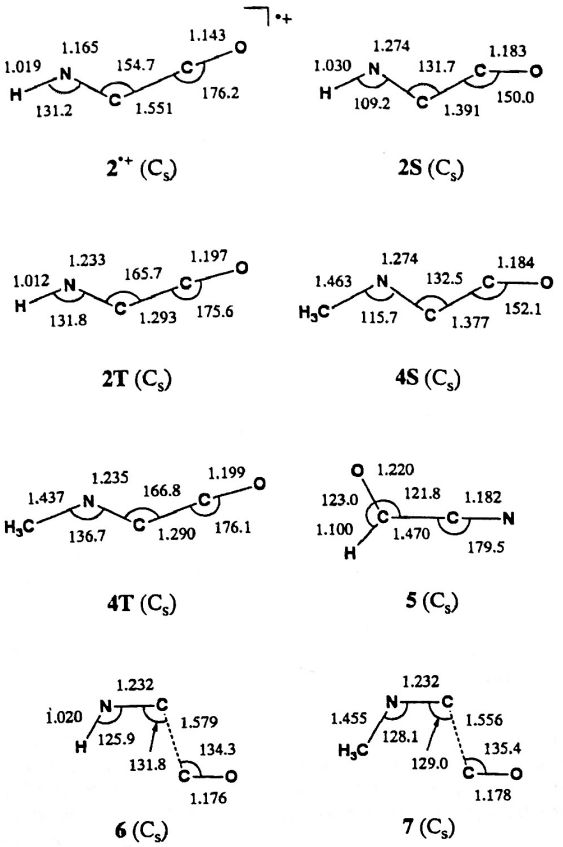

Figure 6. Optimized geometries (MP2/6-31G*) of $C_2HNO^{\bullet+}$, C_2HNO, and C_3H_3NO isomeric structures and transition structures (bond length in angstroms and bond angles in degrees).

distance in $2^{\bullet+}$ (1.551 Å) is significantly longer than that calculated for the sulfur analogue ($HNCCS^{\bullet+}$, 1.333 Å).[8] $2^{\bullet+}$ is predicted to be thermodynamically stable with respect to all possible fragmentations. (Table 1). The energetically most favored reaction corresponds to the loss of a hydrogen atom (endothermic by 225 kJ mol^{-1}). Consistent with the experimental finding, the dissociation channel $2^{\bullet+} \rightarrow HNC^{\bullet+} + CO$ is favored energetically over that forming $HNC + CO^{\bullet+}$. Other fragmentation processes are significantly higher in energy (>500 kJ mol^{-1}). Hence, iminoethenone radical cation ($2^{\bullet+}$) is calculated to be a stable species in the gas phase, in excellent agreement with the experimental observation. The computed adiabatic (IE_a) and vertical (IE_v) ionization energies, at the G2(MP2) level, of HNCCO (**2S**) are 8.94 and 9.31 eV, respectively. The large difference between IE_a and IE_v (0.37 eV) reflects the substantial change in molecular geometry upon ionization (see discussion below).

Relative Energies of C_2HNO Isomers. Several isomeric C_2HNO structures were considered on both the singlet and triplet surfaces. Formyl cyanide, H–CO–CN (**5**), represents the global minimum on the C_2HNO potential energy surface. Iminoethenone, HN=C=C=O (**2S**), an isoelectronic analogue of O=C=C=O,[3] lies 142 kJ mol^{-1} above **5**. The cyclic c-CHNC=O structure has an energy similar to **2S**. Other linear-chain isomers, HOCCN, HCNCO, and HCCNO, are calculated to have higher energy than **2S**, by 49, 61, and 209 kJ mol^{-1}, respectively. As with the sulfur analogue HN=C=C=S,[8] the triplet $^3A''$ state of HNCCO (**2T**) is higher in energy (by 78 kJ mol^{-1}) than the singlet (**2S**). This result is in sharp contrast to other dicarbon cumulene systems O=C=C=O and O=C=C=S, which favor a triplet ground state.[3h,6,22] Several triplet C_2HNO isomers, H(N)CCO, H–CO–CN, HOCCN, HCNCO, and HCCNO, have been considered. Preliminary calculations at the MP2/6-31G* level indicate that their energies are not competitive, and they were not investigated further.

Geometrical Structure of HN=C=C=O. As noted previously for OCCO, SCCS, OCCS, and HNCCS,[3h,7,8,22] the X=C=C=Y systems are generally characterized by rather short central C–C bond (1.28–1.30 Å). A similar C–C bond length is calculated for the triplet HNCCO (**2T**). On the other hand, a significantly longer C–C bond length (1.391 Å) is predicted for the singlet (**2S**), which suggests that **2S** is less stable than other X=C=C=Y analogues. This is readily confirmed by its

TABLE 1: Calculated Total[a,b] (hartrees) and Relative Energies[a] (kJ mol^{-1}) of $HNCCO^{\bullet+}$ ($2^{\bullet+}$), HNCCO (2S), CH_3NCCO (4S), and Related Species

species	sym	state	total energy	rel energy[c]
$HNCCO^{\bullet+}$ ($2^{\bullet+}$)	C_s	$^2A'$	−206.059 57	0
$HNCCO^{\bullet+}$ [d]	C_s	$^2A'$	−206.046 05	35.5
$H(N)CCO^{\bullet+}$	C_s	$^2A'$	−206.046 19	35.1
H–CO–$CN^{\bullet+}$	C_s	$^2A'$	−206.001 51	152.4
$HCNCO^{\bullet+}$	C_s	$^2A'$	−206.053 59	15.7
$HOCCN^{\bullet+}$	C_s	$^2A'$	−206.004 13	145.6
$H^{\bullet}(^2S) + NCCO^+(^1\Sigma^+)$			−205.973 86	225.0
$H^+ + NCCO^{\bullet}(^2A')$			−205.798 18	686.3
$HNC^{\bullet+}(^2\Sigma^+) + CO(^1\Sigma^+)$			−205.955 49	273.3
$HNC(^1\Sigma^+) + CO^{\bullet+}(^2\Sigma^+)$			−205.920 82	364.3
$HN(^1\Sigma^+) + CCO^{\bullet+}(^2\Pi)$			−205.717 44	898.3
$HN^{\bullet+}(^2\Pi) + CCO(^1\Sigma^+)$			−205.660 76	1047.1
$HNCC^{\bullet+}(^2\Pi) + O(^3P)$			−205.696 47	953.3
$HNCC(^1A') + O^{\bullet+}(^2P)$			−205.501 43	1465.4
HNCCO (2S)	C_s	$^1A'$	−206.388 25	0
HNCCO (2T)	C_s	$^3A''$	−206.358 69	77.6
HNCCO[e]	C_s	$^1A'$	−206.349 78	101.0
H–CO–CN (5)	C_s	$^1A'$	−206.442 42	−142.2
c-CHNC=O	C_s	$^1A'$	−206.394 99	−17.7
HCNCO	C_s	$^1A'$	−206.365 06	60.9
HOCCN	C_s	$^1A'$	−206.369 62	48.9
HCCNO	C_s	$^1A'$	−206.308 72	208.8
TS: 2S → HNC + CO (6)	C_s	$^1A'$	−206.382 94	14.0
TS: 2S → 5	C_s	$^1A'$	−206.272 32	304.4
$HNC(^1\Sigma^+) + CO(^1\Sigma^+)$			−206.435 90	−125.1
$H^{\bullet}(^2S) + NCCO^{\bullet}(^2A')$			−206.298 18	236.5
$HN(^3\Sigma^-) + CCO(^3\Sigma^-)$			−205.717 44	550.4
$HNCC(^3A'') + O(^3P)$			−205.696 47	697.4
$HNC(^3A') + CO(^1\Sigma^+)$			−206.211 56	463.9
$HNC(^1\Sigma^+) + CO(^3\Pi)$			−206.298 18	697.4
CH_3NCCO (4S)	C_s	$^1A'$	−245.593 60	0
CH_3NCCO (4T)	C_s	$^3A''$	−245.592 11	82.7
TS: 4S → CH_3NC + CO (7)	C_s	$^1A'$	−245.590 58	7.9
$CH_3NC(^1A') + CO(^1\Sigma^+)$			−245.658 67	−170.8

[a] G2(MP2) E_0 energies. [b] Calculated G2(MP2) E_0 energies include −205.798 18 (NCCO$^{\bullet}$), −205.473 86 (NCCO$^+$), −131.147 56 (HNCC, $^1A'$), −131.143 96 (HNCC, $^3A''$), −130.793 93 (HNCC$^{\bullet+}$), −132.483 27 (CH_3NC), −151.038 57 (CCO, $^3\Sigma^-$), −151.012 49 (CCO, $^1\Sigma^+$), −150.641 92 (CCO$^{\bullet+}$), −93.260 50 (HNC, $^1\Sigma^+$), −93.086 44 (HNC, $^3A'$), −92.780 09 (HNC$^{\bullet+}$), −113.175 40 (CO, $^1\Sigma^+$), −112.951 06 (CO, $^3\Pi$), −112.660 32 (CO$^{\bullet+}$), −55.140 03 (NH, $^3\Sigma^-$), −55.075 53 (NH, $^1\Sigma^+$), −54.655 19 (NH$^{\bullet+}$, $^2\Pi$), −74.978 67 (O, ^3P), and −94.353 98 (O$^{\bullet+}$, ^2P). [c] Relative to $HNCCO^{\bullet+}$ ($2^{\bullet+}$), HNCCO (**2**), and CH_3NCCO (**4**) for $C_2HNO^{\bullet+}$, C_2HNO, and C_3H_3NO species, respectively. [d] Corresponding to vertical ionization of HNCCO. [e] At the equilibrium geometry of $HNCCO^{\bullet+}$.

TABLE 2: Calculated (HF/6-31G*) Vibrational Wavenumbers[a] (cm^{-1}) and Infrared Intensities[b] (km mol^{-1}) of Singlet, Triplet, and Radical Cation of Iminoethenone (2S, 2T and $2^{\bullet+}$)

HNCCO singlet (2S)			HNCCO triplet (2T)			$HNCCO^{\bullet+}$ ($2^{\bullet+}$)		
A′	3453	(877)	A′	3299	(11)	A′	3411	(113)
	2284	(8)		2042	(767)		2178	(305)
	1917	(165)		1685	(115)		1628	(287)
	656	(77)		1170	(267)		911	(17)
	616	(151)		700	(11)		689	(587)
	495	(4)		315	(5)		407	(18)
	178	(0)		230	(58)		240	(9)
A″	720	(168)	A″	907	(105)	A″	301	(7)
	273	(0)		254	(0)		239	(25)

[a] Scaled by a factor of 0.8929 (ref 21). [b] Intensity values are in parentheses.

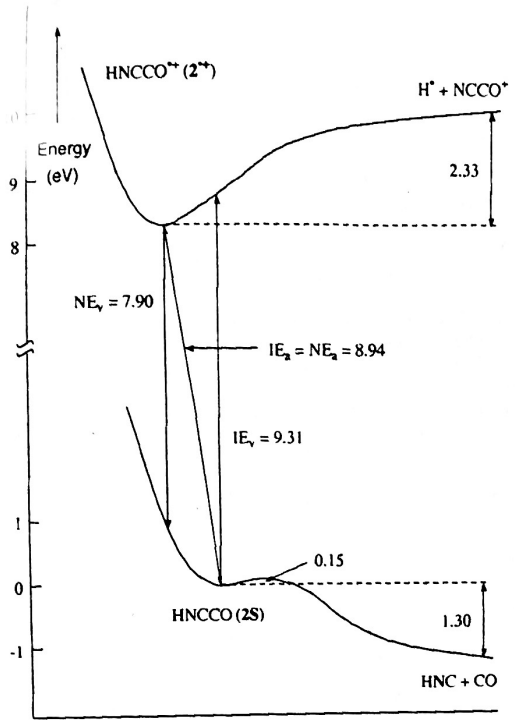

Figure 7. Schematic potential energy surfaces for the fragmentation of HNCCO (**2S**) and HNCCO•+ (**2**•+) showing neutralization and ionization processes (NE_v = vertical neutralization energy, NE_a = adiabatic neutralization energy, IE_v = vertical ionization energy, and IE_a = adiabatic ionization energy).

calculated stability (see discussion below). Note that the electrons of the N=C=C=O skeleton in **2S** are considerably more delocalized than the corresponding radical cation (**2**•+). The C–N and C–O bond distances are longer (by 0.04–0.10 Å), while the C–C bond length is shorter (by 0.16 Å).

Stability of HN=C=C=O. To assess the stability of iminoethenone in the gas phase, we have examined all possible (spin-allowed) unimolecular fragmentation processes of **2S**. The energy requirement for these reactions are summarized in Table 1. In contrast to the sulfur analogue (HNCCS),[8] the energetically most favorable fragmentation reaction of **2S**, the loss of CO, is calculated to be exothermic, by 125 kJ mol^{-1}. The other dissociation reactions of **2S**, leading eventually to H•, O, or NH, are predicted to be endothermic, by 237, 550, and 697 kJ mol^{-1}, respectively. Decomposition of **2S** to HNC + CO is calculated to have a small barrier of 14 kJ mol^{-1}, proceeding via transition structure **6** (Figure 6). This small calculated barrier is consistent with the fact that the C···C distance in **6** (1.579 Å) is rather short, compared to that calculated for HNCCS (1.862 Å; barrier = 120 kJ mol^{-1}).[8] Thus, iminoethenone (**2S**) is unlikely to be an observable species. Unimolecular rearrangement of **2S** to formyl cyanide (**5**), via a 1,3-hydrogen shift, requires a high activation barrier of 304 kJ mol^{-1} (but such a process could take place easily as a bimolecular or wall-catalyzed reaction as in the case of HNCCS).[8] For the triplet HNCCO (**2T**), the spin-allowed dissociations to HNC($^3\Pi$) + CO($^1\Sigma^+$) or HNC($^1\Sigma^+$) + CO($^3\Pi$) are predicted to be endothermic by 254 and 386 kJ mol^{-1}, respectively. Therefore, triplet iminoethenone is predicted to be an experimentally accessible species in the gas phase.

Neutralization in an NR experiment is generally considered as a vertical process.[10] Thus, it is instructive to calculate the energy for the vertically neutralized species (NE_v) of HNCCO. Our calculations show that vertical neutralization of ground-state HNCCO•+ (**2**•+) should lead to neutral HNCCO (singlet) molecules with 101 kJ mol^{-1} internal energy, due to a large change in geometry in going from HNCCO•+ (**2**•+) to HNCCO (**2S**) (see Figure 7). This energy is well above the energy required (14 kJ mol^{-1}) for the dissociation of **2S** to HNC + CO. Hence, our calculated results are consistent with the experimental finding that iminoethenone is not observable in the NR mass spectrum.

Structure and Stability of CH_3N=C=C=O. As with the parent compound (**2**), (methylimino)ethenone (**4**) is predicted to have a singlet ground state. The singlet–triplet gap is slightly larger (83 kJ mol^{-1}). The calculated N–C, C–C, and C–O bond lengths in **4S** and **4T** (Figure 5) are similar to those calculated for **2S** and **2T**, respectively. Decomposition of **4S** to CH_3NC + CO is calculated to be exothermic (by 171 kJ mol^{-1}) and inhibited by an activation barrier of just 8 kJ mol^{-1}, via transition structure **7** (Figure 6). Therefore, **4S** is also predicted not to be a readily observable species in the gas phase, in good accord with the experimental finding.

4. Conclusions

The iminoethenone radical cations **2**•+ and **4**•+ are stable in the gas phase on the time scale of the mass spectrometry experiments. On the other hand, the neutral cumulenes **2** and **4** are not accessible by NRMS experiments, in sharp contrast to their sulfur analogues, RN=C=C=S. Ab initio calculations, at the G2(MP2) level of theory, demonstrated that the neutral iminoethenones (**2** and **4**) exist in energy wells of only ~10 kJ mol^{-1} with respect to CO loss. As with RNCCS, both **2** and **4** are predicted to have singlet ground states. Iminoethenone radical cation (**2**•+) is predicted to be the global minimum on the $C_2HNO^{\bullet+}$ potential energy surface.

5. Experimental Section

The electron impact mass spectra were recorded on a large-scale tandem mass spectrometer combining six sectors (VG Analytical AutoSpec 6F; VG Analytical, Manchester, UK) of $E_1B_1E_2E_3B_2E_4$ geometry (E electric sector, B magnetic sector) operating at an accelerating voltage of 8 kV.[23] In the CA experiments, a beam of ions is mass selected by the combination of the first sectors ($E_1B_1E_2$) and submitted to collisional activation with helium or oxygen (80% transmission). In the MS/MS/MS experiments, the two collision gases used in sequence were helium and oxygen. In the NR experiments, neutralization of the ions with ammonia (80% transmission) precedes reionization with oxygen, unreacted ions being eliminated by floating the intermediate calibration ion source inserted between the two cells at 9 kV. The spectra were recorded by scanning E_3 and collecting the ions in the fifth field-free region.

Compound **1** was prepared according to the literature.[24] Compounds **3** and **3D** were prepared by methylation of **1** with dimethyl sulfate [$(CD_3)_2SO_4$ for **3D**] using a procedure described by Schmidt et al.[25] **3**: mp 164–168.5 °C, ^{1}H NMR (DMSO-d_6, 300 MHz) δ 7.7 (m, 5 H), 3.4 (s, 3 H), 3.2 (s, 3 H).

Acknowledgment. We are grateful for financial support of this research by the Australian Research Council (ARC). M. W. Wong thanks the ARC for the award of an Australian Research Fellowship. R. Flammang thanks the Fonds National de la Recherche Scientifique for its contribution toward the acquisition of the VG AutoSpec 6F mass spectrometer. We also thank Prof. J. K. Terlouw for useful comments.

References and Notes

(1) Weltner, W. W., Jr.; Van Zee, R. J. *Chem. Rev.* **1989**, *89*, 1713.
(2) (a) Sülzle, D.; Schwarz, H. *Chem. Ber.* **1989**, *122*, 1803. (b) Hirahara, Y.; Susuki, H.; Yamamoto, S.; Kawaguchi, K.; Karfu, N.; Chishi, M.; Takano, S.; Ishikawa, S.-I.; Masuda, A. *Astrophys. J.* **1992**, *394*, 539 and references therein.
(3) (a) Strating, J.; Zwanenburg, B.; Wagenaar, A.; Udding, A. C. *Tetrahedron Lett.* **1969**, 125. (b) Haddon, R. D. *Tetrahedron Lett.* **1972**, 3897. (c) Fleischhauer, J.; Bechers, M.; Scharf, H.-D. *Tetrahedron Lett.* **1973**, 4275. (d) Knight, L. B., Jr.; Steadman, J.; Miller, P. K.; Bowman, D. E.; Davidson, E. R.; Feller, D. *J. Chem. Phys.* **1984**, *80*, 4393. (e) Birney, D. M.; Berson, J. A. *Tetrahedron* **1986**, *42*, 1561. (f) Berson, J. A.; Birney, D. M.; Dailey, W. P.; Leibman, J. F. In *Molecular Structure and Energetics*;

Liebman, J. F., Greenberg, A., Eds.; VCH Publishers: Weinheim, Germany, 1988; Vol. 6. (g) Plisnier, M. Ph.D. Thesis, University of Mons-Hainaut, Belgium, 1992. (h) Sülzle, D.; Weiske, T.; Schwarz, H. *Int. J. Mass Spectrom. Ion Processes* **1993**, *125*, 75.

(4) (a) Maier, G.; Reisenauer, H. P.; Schrot, J.; Janoschek, R. *Angew. Chem., Int. Ed. Engl.* **1990**, *29*, 1464.

(5) Wentrup, C.; Kambouris, P.; Evans, R. A.; Owen, D.; Macfarlane, G.; Chuche, J.; Pommelet, J. C.; Ben Cheikh, A.; Plisnier, M.; Flammang, R. *J. Am. Chem. Soc.* **1991**, *113*, 3130.

(6) Sülzle, D.; Schwarz, H. *Angew. Chem., Int. Ed. Engl.* **1988**, *27*, 1337.

(7) Sülzle, D.; Terlouw, J. K.; Schwarz, H. *J. Am. Chem. Soc.* **1990**, *112*, 628.

(8) Flammang, R.; Landu, D.; Laurent, S.; Barbieux-Flammang, M.; Wong, M. W.; Kappe, C. O.; Wentrup, C. *J. Am. Chem. Soc.* **1994**, *116*, 2005.

(9) Levsen, K.; Schwarz, H. *Angew. Chem., Int. Ed. Engl.* **1976**, *15*, 509.

(10) For reviews, see: (a) Wesdemiotis, C.; McLafferty, F. W. *Chem. Rev.* **1987**, *87*, 485. (b) Terlouw, J. K.; Schwarz, H. *Angew. Chem., Int. Ed. Engl.* **1987**, *26*, 805. (c) Holmes, J. L. *Mass Spectrom. Rev.* **1989**, *8*, 513. (d) McLafferty, F. W. *Science* **1990**, *247*, 925. (e) Plisnier, M.; Flammang, R. *Chim. Nouv.* **1990**, *8*, 893.

(11) Hehre, W. J.; Radom, L.; Schleyer, P. v. R.; Pople, J. A. *Ab Initio Molecular Orbital Theory*; Wiley: New York, 1986.

(12) (a) Curtiss, L. A.; Raghavachari, K.; Pople, J. A. *J. Chem. Phys.* **1993**, *98*, 1293. (b) Curtiss, L. A.; Raghavachari, K.; Trucks, G. W.; Pople, J. A. *J. Chem. Phys.* **1991**, *94*, 7221.

(13) Lias, S. G.; Bartmess, J. E.; Liebman, J. F.; Holmes, J. L.; Levin, R. D.; Mallard, W. G. *J. Phys. Chem. Ref. Data* **1988**, *17* (Suppl. 1).

(14) (a) Burgers, P. C.; Holmes, J. L.; Mommers, A. A.; Terlouw, J. K. *Chem. Phys. Letts.* **1983**, *102*, 1. (b) McLafferty, F. W.; McGilvery, D. C. *J. Am. Chem. Soc.* **1980**, *102*, 6189. (c) A referee has objected that, because $HNC^{\bullet+}$ cation corresponds to the global minimum of the $[HCN]^{\bullet+}$ potential energy surface, sufficient energy could be supplied in the first CA process to overcome the ~170 kJ mol^{-1} barrier for isomerization of $HCN^{\bullet+}$ to $HNC^{\bullet+}$ irrespective of the original connectivity. This possibility cannot be rejected out of hand since we show elsewhere (see below) that post-collisional isomerizations are possible for other ions. Although ~170 kJ mol^{-1} is significant barrier, we have attempted to demonstrate such an isomerization, so far without success. Thus, HCN was ionized and its CA (O_2) spectrum recorded. This spectrum (m/z 12–15) is not modified by pressurizing the intermediate collision cell with He so as to reduce the intensity of the ion signal to 50% before the collision with O_2. Precursors for strong $HCN^{\bullet+}$ signals in CA spectra are being sought. The question obviously requires further study.

(15) (a) Examples of NRMS being more characteristic than CAMS are $C_nHS^{\bullet+}$ ions (e.g., $HCCCS^+$) and $RNC_3S^{\bullet+}$ (e.g., $CH_3NCCCS^{\bullet+}$): Flammang, R.; Wong, M. W.; Wentrup, C., to be published; $C_3HO_2^+$: Morizur, J. P.; Provot, G.; Tortajada, J.; Gal, J.-F.; Maria, P.-C.; Flammang, R.; Van Haverbeke, Y. *Int. J. Mass Spectrom. Ion Processes*, submitted; and $HNS^{\bullet+}$ and H_2NS^+. (b) The phenomenon of post-collisional isomerization is potentially very important and merits further investigation. The $[M-H]^+$ ion from ketene ($CH_2{=}C{=}O$) is an obvious candidate for study of m/z 41 ions. The molecular ion of ketene itself (m/z 42) also loses CH to give m/z 29, again a likely post-collisional process. (c) Further work is also aimed at understanding the collision gas effect (O_2 versus He) in this and other examples. Prof. J. K. Terlouw (McMaster University, Canada) has informed us of the operation of a collision gas effect in the CA spectra of $[M-CH_3]^+$ ions from 2-propanol. (c) Note that the nitrene ion $H(N)C{=}C{=}O^{\bullet+}$ is calculated to be relatively stable, whereas $H{-}CO{-}CN^{\bullet+}$ is significantly higher in energy than $HNCCO^{\bullet+}$ (section 3). However, further experimental studies of these isomeric ions are desirable.

(16) McGibbon, G. A.; Kingsmill, C. A.; Terlouw, J. K.; Burgers, P. C. *Int. J. Mass Spectrom. Ion Processes* **1992**, *121*, 11.

(17) Loss of CO is not a metastable process, and a significant contribution of collisionally induced dissociative ionization (CIDI) to the NRMS seems unlikely. The $HNCCO^{\bullet+}$ ions are extremely stable toward unimolecular fragmentations; averaging of more than 100 scans was required in order to obtain an acceptable metastable ion (MIKE) spectrum of $HNCCO^{\bullet+}$, which features just two peaks, m/z 27 and 54, with comparable intensities.

(18) Parmentier, M.; Galloy, J.; Van Meersche, M.; Viehe, H. G. *Angew. Chem., Int. Ed. Engl.* **1975**, *14*, 53.

(19) The molecular dication, CH_3NCCO^{2+}, is calculated not to be a stable species, dissociating spontaneously to $CH_3NC^{\bullet+} + CO^{\bullet+}$ upon geometry optimization. On the other hand, the $[M-H_2]$ dication, $HCNCCO^{2+}$, is predicted to be a kinetically stable species, in excellent agreement with its observation in CAMS of $CH_3NCCO^{\bullet+}$.

(20) Frisch, M. J.; Trucks, G. W.; Head-Gordon, M.; Gill, P. M. W.; Wong, M. W.; Foresman, J. B.; Johnson, B. G.; Schlegel, H. B.; Robb, M. A.; Replogle, E. S.; Gomperts, R.; Andres, J. L.; Raghavachari, K.; Binkley, J. S.; Gonzalez, C.; Martin, R. L.; Fox, D. J.; DeFrees, D. J.; Baker, J.; Stewart, J. J. P.; Pople, J. A. *GAUSSIAN 92*; Gaussian Inc.: Pittsburgh, PA, 1992.

(21) Pople, J. A.; Scott, A. P.; Wong, M. W.; Radom, L. *Isr. J. Chem.* **1993**, *33*, 345.

(22) (a) Raine, G. P.; Schaefer, H. F., III; Haddon, R. C. *J. Am. Chem. Soc.* **1983**, *105*, 194. (b) Janoschek, R. *J. Mol. Struct. (THEOCHEM)* **1991**, *232*, 147.

(23) Bateman, R. H.; Brown, J.; Lefevere, M.; Flammang, R.; Van Haverbeke, Y. *Int. J. Mass Spectrom. Ion Processes* **1992**, *115*, 205.

(24) Desimoni, G.; Grünanger, P. *Gazz. Chim. Ital.* **1966**, *96*, 25.

(25) Schmidt, P.; Eichenberger, K.; Wilhelm, M.; Druey, J. *Helv. Chim. Acta* **1959**, *62*, 49.